Ornamental Horticulture
ISSN 2447-536X | WWW.ORNAMENTALHORTICULTURE.COM.BR
SBFPO Sociedade Brasileira de Floricultura e Plantas Ornamentais

ARTICLE

Genome and karyotype differences between diploid and tetraploid desert roses

Diferenças genômicas e cariotípicas em variedades diploides e tetraploides de rosa-do-deserto

Talita Angélica de Oliveira Rosa[1], Juliana Machado da Silva[1], Thamirys Silva Valentim[1], Rafael de Assis[1], Letícia Maria Parteka[1], André Luís Laforga Vanzela[1,*]

[1]Universidade Estadual de Londrina, Londrina-PR, Brasil

Abstract
Adenium (Apocynaceae) is a genus that contains succulent species, with sculptural stems and large variations in flower shapes and colors. Most of the world's production chain consists of hybrids, and *A. obesum* (2*n* = 22) is the species with the greatest ornamental interest. *Adenium arabicum* (2*n* = 44) and *A. obesum* differ in their morphological characteristics and are found in distinct geographical areas. According to botanical nomenclature rules, *A. arabicum* should be named *A. obesum* or a variety thereof. However, this may be genetically questionable. Although genetic variation data for desert roses is scarce, it is crucial for the ornamental plant production sector. The objective of this study was to use data from flow cytometry, karyotype and nucleus characterization, repetitive DNA fraction, bioinformatic tools and physical location of sequences by in situ hybridization to improve understanding of genomic diversity among diploid and tetraploid *A. obesum* varieties. The karyotypes were composed of meta- and submetacentric chromosomes, and the genome size ranged from 2C = 1.98 pg in diploid samples to 2C = 2.92 pg in tetraploid samples. Chromosome banding revealed similarities between the varieties, with the accumulation of AT-rich regions ($DAPI^+$) bands present in the proximal-interstitial chromosome regions, and a smaller number of GC-rich regions (CMA^+). The $DAPI^+$ and CMA^+ regions, along with ribosomal DNA and Gypsy retrotransposons, predominated in the interphase chromocenters. Differences in the morphology, chromosome number, *in situ* hybridization signals, and the DNA C-value between these two groups of samples reinforces that they are distinct species and not varieties. Particularly since it would be very difficult to obtain regular meiosis from the crossing of two different sets of chromosomes. Such information is important for the genetic improvement of desert roses.
Keywords: CMA/DAPI bands, chromocenters, DNA C-value, polyploidy, ribosomal DNA.

Resumo
Adenium (Apocynaceae) é um gênero de espécies suculentas, com caules esculturais e grandes variações nas formas e cores das flores. A maior parte da cadeia de produção mundial consiste em híbridos, e *A. obesum* (2*n* = 22) é a espécie com maior interesse ornamental. *Adenium obesum* e *A. arabicum* (2*n* = 44) diferem em suas características morfológicas e são encontrados em áreas geográficas distintas. De acordo com as regras de nomenclatura botânica, *A. arabicum* deveria ser chamado por *A. obesum* ou uma variedade dele. No entanto, isso pode ser geneticamente questionável. Embora os dados de variação genética para as rosas do deserto sejam escassos, eles são cruciais para o setor de produção de plantas ornamentais. O objetivo deste estudo foi usar dados de citometria de fluxo, caracterização dos cariótipos e núcleos, porção repetitiva de DNA, bioinformática e localização física de sequências por hibridização *in situ*, para melhorar a compreensão da diversidade genômica entre variedades diploides e tetraploides de *A. obesum*. Os cariótipos foram compostos por cromossomos meta e submetacêntricos, e o tamanho dos genomas variou de 2C = 1,98 pg em amostras diploides a 2C = 2,92 pg em amostras tetraploides. O bandeamento cromossômico revelou similaridades entre as variedades, com o acúmulo de bandas de regiões ricas em bases AT ($DAPI^+$) presentes nas regiões cromossômicas intersticiais-proximais, e uma quantidade menor de regiões ricas em bases GC (CMA^+). As regiões $DAPI^+$ e CMA^+, juntamente com o DNA ribossômico e os retrotransposons Gypsy, predominaram nos cromocentros na interfase. Diferenças na morfologia, número de cromossomos, sinais de hibridização *in situ* e de redução do valor C do DNA entre esses dois grupos de amostras, reforçam a ideia de que são espécies diferentes e não variedades. Principalmente porque seria muito difícil obter meiose regular a partir do cruzamento de dois conjuntos diferentes de cromossomos. Essas informações são importantes para o melhoramento genético das rosas do deserto.
Palavras-chave: bandas CMA/DAPI, conteúdo de DNA, cromocentros, DNA ribossômico, poliploidia.

Introduction

Adenium (Forssk.) Roem. & Schult. (Apocynaceae) is a genus from the semi-arid regions of Africa and the Arabian Peninsula. Together with *Nerium* L., it comprises the Nerium clade. They share similar floral morphology, with extremely long and pubescent anther connectives, and seeds containing both micropylar and chalazal comas (Fishbein et al., 2018). *Adenium* species are succulents typical of savannas and open forests with sandy or rocky soils, a sculptural stem, and variations in flower shape and color. These morphological characteristics give *Adenium* a high commercial value as an ornamental plant (Colombo et al., 2018).

Some desert rose breeders use the name *Adenium arabicum* Balf.f. to differentiate between larger and smaller plants, which are named after *A. obesum* (Forssk.) Roem. & Schult., although this taxonomic conflict has already been mentioned in the literature (Hastuti et al., 2009; Dimmit and Edwards, 2021). *Adenium arabicum*, first published as *Nerium obesum* Forssk. in 1775, occurs in Saudi Arabia and Yemen, but was renamed *A. obesum* Roem. & Schult. in 1819. Attempts to cross *A. obesum*, which is diploid with 2*n* = 22, with the larger *A. arabicum*, which is probably polyploid with 2*n* = 44, usually result in unsuccessful crosses. Following nomenclatural rules and Dimmit and Edwards (2021), we prefer to consider both to be varieties of *A. obesum*.

Das et al. (1999) reported karyotype differences based on the number and length of chromosomes and estimates of the amount of nuclear DNA (4C) in some species of *Adenium*. *Adenium swarzicum* Stapf and *A. arabicum* Balf. f., both with 2*n* = 44, could be tetraploid (Dimmit and Edwards, 2021). In addition, interspecific variations in chromosome sizes and shapes, karyotype symmetry, and genomic DNA content were observed by Dimmit and Edwards (2021). As genomic and cytogenetic data can be useful for resolving taxonomic conflicts, we used cytogenomic and flow cytometry tools to identify differences between *A. obesum* and *A. arabicum*. The majority of *A. obesum* plants produced in Brazil and worldwide are hybrids (Colombo et al., 2018). Because of this, recognition and taxonomic delimitation of samples and species that originate from Africa are crucial. It is possible that this information will support our hypothesis that *A. obesum* and *A. arabicum* are two distinct taxonomic entities. Moreover, these data could clarify the difficulties that arise from interspecific crossbreeding that occur in the flower production industry.

***Corresponding author:** andrevanzela@uel.br | https://doi.org/10.1590/2447-536X.v31.e312810 | Editor: Maurecilne Lemes da Silva Carvalho, Universidade do Estado de Mato Grosso, Brasil | Received: Sep 01, 2024 | Accepted: Apr 08, 2025 | Available online: May 07, 2025 |

Material and Methods

Plant material

Samples of *A. obesum* with 2*n* = 22 (the diploid varieties named TS001 and TS002) and those with 2*n* = 44 (tetraploid varieties TS013 and TS014) were imported from natural populations of Africa and maintained by the Flora Takemura Company (FTC), Distrito da Warta, Londrina, Paraná, Brazil. Twenty living samples of each cultivar were kept at the Laboratory of Cytogenetics and Plant Diversity, State University of Londrina, Paraná, Brazil, to allow the collection of biological material. Biological samples have been collected during the years 2021 and 2022. Images of each diploid and tetraploid are shown in the Figs. 1 and 2. None of the samples underwent crossing cycles and all vouchers were stored at FTC.

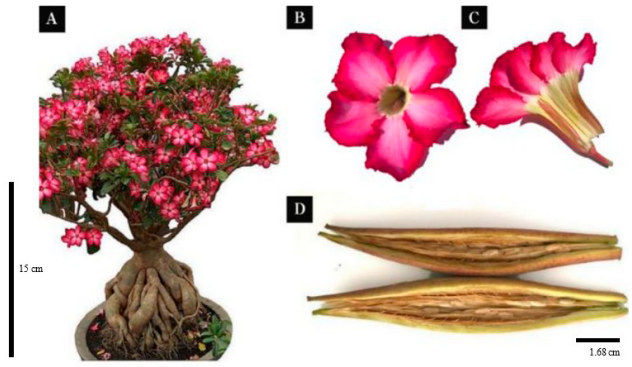

Fig. 1. Morphological characteristics of the diploid variety (*A. obesum*), which has a succulent herbaceous habit, ~30 cm tall, with a sculptural and variable stem (1A). It has dark green deciduous leaves, with dichlamydeous and pentamerous flowers of varying colour and shape (1B and 1C). The seeds are winged and the capsules have an average length of 10 cm (1D). The stamens are conical and the anthers have slits facing the stigma. The ovary is syncarpous and the fruit is apocarpic and capsule-like with ~200 seeds, opening longitudinally along the line where the carpels join. Photographs by Talita A. O. Rosa.

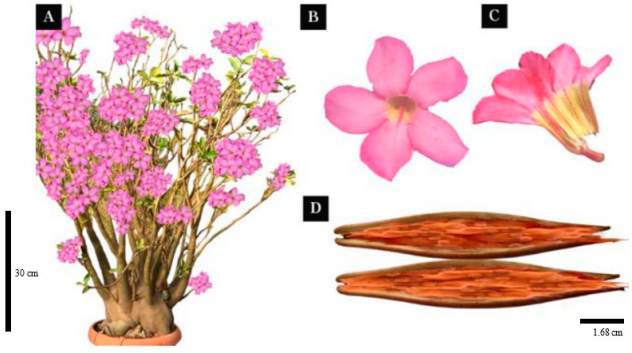

Fig. 2. Morphological characteristics of the tetraploid variety (*A. arabicum*), with a height of about 90 cm or more (2A), which differs from others in that it has a spherical stem with branches that grow from the base of the stem. The leaves are hairy and the flowers are pale pink (2A and 2C). The seeds are up to three times larger than those of other *Adenium* species (2D). Photographs by Talita A. O. Rosa.

DNA C-value estimates

The nuclear DNA contents of diploid and tetraploid samples of *A. obesum* were measured and compared according to the procedure of Praça-Fontes et al. (2011), with small modifications including the standards. Three genomes that are considered to be excellent standards for use in plant flow cytometry (Temsch et al., 2022), *Solanum lycopersicum* L. var. Stupické, Solanaceae (2C = 1.96 pg), *Raphanus sativus* (2C = 1.11 pg), and *Pisum sativum* L. 'Ctirad', Fabaceae (2C = 9.09 pg) were used. Young leaves were chopped in 250 µL of OTTO-I buffer containing polyethylene glycol (PEG) (7%) and RNase (1 mg mL^{-1}). Samples were filtered through a 30 µm nylon mesh and centrifuged at 500 *xg*. Subsequently, the nuclei were stained with OTTO-I: OTTO-II buffer, 1:2 (v v^{-1}) containing polyethylene glycol (7%), RNase (1 mg mL^{-1}), and propidium iodide (1 mg mL^{-1}). Samples were filtered again through a 20 µm nylon mesh. Measurements were performed using a BD Accuri C6 flow cytometer (Becton Dickinson and Company). Three independent estimations were performed at two-day intervals. Measurements of at least 5,000 nuclei were taken in each reading cycle (three times). The 2C values were calculated as sample peak mean/standard peak mean × amount of 2C DNA of standard (pg).

Genomic analysis

The search for sequenced genomes in open access databases found only sequences of *A. obesum*. They were obtained from NCBI (SRA accession ERR5033363). To track stretches of repetitive sequences, paired-end reads were filtered with a quality cutoff 10, with 95% of bases above the cutoff point, interlaced, and overlapped with a minimum length of 30 nt. The RepeatExplorer/TAREAN pipeline (Novak et al., 2017) was used with default parameters. TAREAN output files were used to organize potential satDNA families. Transposable Elements (TEs) were evaluated using databases of conserved domains from GypsyDB (https://gydb.org/) and RexDB (http://repeatexplorer.org/). Additionally, these sequences were compared with the NCBI conserved domains database (http://www.ncbi.nlm.nih.gov). To evaluate the proportion of 35S and 5S rDNA, a database composed of 1,652 sequences from various organisms was compiled from NCBI and used in a local BLASTn, maintaining > 80% identity and max_target_seqs 1 as parameters.

DNA extraction, PCR, and probes

To obtain a greater number of cells, nuclear DNA was isolated from the young leaves of each sample using CTAB buffer (Schenk et al., 2023). The samples were purified with phenol:chloroform (1:1, v v^{-1}) and chloroform:isoamyl alcohol (24:1, v v^{-1}) twice, treated with RNase (1 mg mL^{-1}), precipitated in 100% absolute ethanol, and eluted in 10 mM Tris-HCl (pH 8.0). The concentrations were estimated using a NanoDrop 2000 Spectrophotometer (Thermo Sci).

The 35S ribosomal probe was labeled with biotin-11-dUTP using nick translation kits (Jena Bioscience) and 5S labeled by PCR using the primers UP46-F 5′GTGCGATCATACCAGCRYTAATGCACCGG and UP47-R 5′ GAGGTGCAACACGAGGACTTCCCAGGAGG, with Cy3-dUTP (Sigma). Both procedures were according to Souza et al. (2020), using genomic DNA from diploid samples of *A. obesum*. For this, PCR was conducted using a mix containing 2 mM $MgCl_2$, 0.4 µM of each primer, 0.2 mM dNTP, ~ 30 ng DNA template, 1.25 U of Taq polymerase, and ultrapure water to complete 25 µL. Probes were labeled using 0.2 mM dNTPs, containing dGTP (25%), dCTP (25%), dATP (25%), dTTP (17.5%), biodUTP (7.5%) or Cy3-dUTP (7.5%). The PCR was conducted under the following cycling conditions: 94 °C for 3 minutes, 30 cycles of denaturation at 94 °C for 1 minute, 50 °C for 30 seconds, 72 °C for 1 minute, and a final extension at 72 °C for 10 minutes.

Sequences with ≥ 90% identity for the reverse transcriptase of Gypsy LTR-retrotransposons were used to design primers (RT_Gypsy_Forward-1, RT_Gypsy_Forward-2, and RT_Gypsy_Reverse-1), which can be seen in Table 1, as well as the regions of the RT sequence alignment (Fig. 3). These primers were used in a semi-nested PCR method to specifically amplify Gypsy-derived amplicons. Initially, PCR was performed using RT_Gypsy_F-1 + RT_Gypsy_R-1 primers. A band ~200 bp in length was cut from the agarose gel, purified with the PureLink™ PCR Purification Kit (Thermo Fisher), and re-amplified using RT_Gypsy_F-2 + RT_Gypsy_R-1 primers. The resulting ~200 bp amplicon from this second reaction was reamplified in a new PCR containing Cy3-dUTP. The following standard PCR was used: 5 U μL^{-1} Taq polymerase (0.5 µL), 10× buffer (2.5 µL), 50 mm $MgCl_2$ (1.5 µL), 10 mm dNTP (1 µL), 5 mm primers (2 µL each), and H_2O up to a final volume of 25 µL, using the following conditions: 94 °C for 2 minutes, 30 cycles of 94 °C for 40 seconds, 59 °C for 40 seconds, and 72 °C for 1 minutes, and a final extension of 72 °C for 10 minutes. All reactions were tested using electrophoresis in an agarose gel at 3 V/cm and stained with ethidium bromide.

Table 1. Primers designed for semi-nested PCR to obtain a 200 bp amplicon using as template DNA extracted from *Adenium obesum*.

Primers	Sequences
RT_Ogre_Forward-1	CCTTTGAAGTGTGCATTTGG
RT_Ogre_Forward-2	TTGGGTTTCATTGTGCGACA
RT_Ogre_Reverse-1	TCAAATCTTGCTGGACGATG

Fig. 3. Gypsy/Ogre retrotransposon reverse transcriptase sequence for which primers were obtained and designed.

Cytogenetic analysis

Chromocenters per interphase nuclei, chromosome size and shape, and the general organization of karyotypes were used to compare samples of diploid and tetraploid varieties. Root tip meristems, which are undergoing intense cell division, were selected to obtain a good number of mitotic metaphases. Roots were pretreated with a saturated solution of paradichlorobenzene for 2 hours at room temperature to block the cell cycle in the metaphase phase. The samples were then fixed in ethanol:acetic acid (3:1, v v^{-1}). For conventional analyses, samples were treated in 1M HCl at 60 °C for 10 minutes and squashed in a drop of 60% acetic acid. After liquid nitrogen freezing, the coverslips were removed, and the slides were air-dried and stained with 2% Giemsa. Young anthers were used to observe chromosomes during meiosis. For that, samples were fixed in ethanol:acetic acid (3:1, v v^{-1}), hydrolyzed in 5 M HCl for 20 minutes at room temperature, and squashed as described above. Each variety had its somatic chromosome numbers determined in at least ten metaphases. Chromosome types were classified as metacentric, submetacentric, and acrocentric, according to Vimala et al. (2021).

For CMA/DAPI banding and FISH, samples were treated in a solution of 2% cellulase and 20% pectinase at 37 °C for 2 - 4 hours and squashed in a drop of 60% acetic acid. Slides were stained with 0.5 mg mL^{-1} CMA_3 (chromomycin A_3) for 90 minutes, followed by staining with 2 mg mL^{-1} DAPI (4-6-diamidino-2-phenylindole) for 30 minutes, and mounted in a solution of 90% glycerol, 1% 2.5 mM $MgCl_2$ and 90% McIlvaine buffer (pH 7.0), such as described by Barreto et al. (2023). For better fixation of chromosomes and nuclei on the slide and thus offering resistance to subsequent treatments, preparations were stored for at least three days before analysis at room temperature. At least 30 cells were analyzed for each sample.

Fluorescence *in situ* hybridization (FISH) was performed as described by Barreto et al. (2023). Probes were utilized in a mixture of 34 µL containing 100% formamide (15 µL), 50% PEG (6 µL), 20× saline-sodium citrate (SSC) (3 µL), 100 ng of calf thymus DNA (1 µL), 10% sodium dodecyl sulfate (SDS) (1 µL), 200 ng of probes (4 µL), and distilled water to complete the mixture. The material was denatured at 90 °C for 10 minutes, and hybridization was performed at 37 °C overnight in a humid chamber. Post-hybridization washes were carried out using ~70% stringency with three washes in the SSC buffer. The 35S rDNA probe was detected with avidin-FITC. Post-detection washes were performed at room temperature in 4× SSC/0.2% Tween 20. Slides were mounted with 25 µL of antifade medium, plus 4 µL of 2 µg mL^{-1} DAPI.

Results

Differences in karyotypes and DNA content between diploid and tetraploid samples

The results from conventional cytogenetics showed well-defined chromocenters in interphasic nuclei, which varied in size within and between nuclei (Figs. 4A and B, 4E, 4F and 4G). Chromosomes are very small and difficult to analyze. Chromosome shapes and primary constrictions could only be identified by measuring in µm (Fig. 5). Diploid and tetraploid samples exhibited asymmetric karyotypes, with evident differences in chromosome sizes. Diploid samples of *A. obesum* seem to be meta- and submetacentric chromosomes, presenting $2n = 2x = 22$ with 6 m + 5 sm and regular meiosis with bivalents (Figs. 1C and 1D), while $2n = 4x = 44$ (20 m + 2 sm) was observed in the tetraploid (Fig. 1H). The chromosomes of the diploid ranged from 1.25 to 2.45 µm in length and had a total chromosome length of 20.82 µm (Fig. 5), while in the tetraploid, they ranged from 0.95 to 1.86 µm, and the total chromosome length was 30.71 µm (Fig. 5). The chromosome length in the tetraploid was 67.8% larger than that in the diploid (about 25% smaller than expected for an autotetraploid genome, which hypothetically should be close to 41.64 µm).

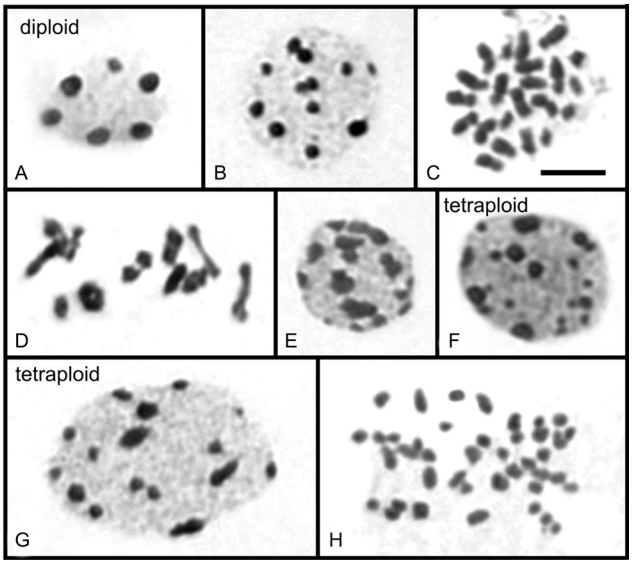

Fig. 4. Cytogenetic analysis in diploid and tetraploid samples of *A. obesum*. (4A, 4B and 4E) Interphase nuclei with variation in the number of chromocenters in the diploid variety. (4C) Mitotic metaphase with 22 chromosomes in the diploid. (4D) Diakinesis with 11 bivalents in the diploid. (4F and 4G) Interphase nuclei with variation in the number of chromocenters in the tetraploid. (4H) Mitotic metaphase with 44 chromosomes in the tetraploid. The bar represents 10 µm.

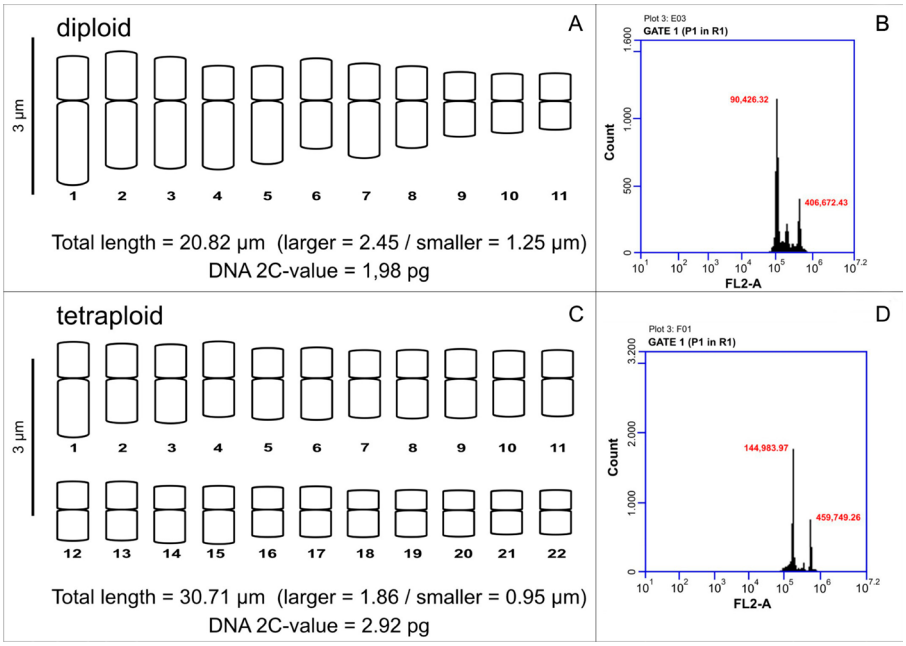

Fig. 5. Karyotypes and flow cytometry data for diploid (5A) and tetraploid (5C) *A. obesum*. Note that both karyotypes are relatively asymmetric, that the largest chromosomes are twice as large as the smallest, and that the DNA C values are clearly contrasting. Flow cytometry data show 2C values, with the largest peaks representing G1 and the smallest ones in G2. The intermediate peaks correspond to the standard (*P. sativum*), for the diploid (5B) and tetraploid (5D) samples.

Cytometry assays showed that 2C values ranged from 2C = 1.98 pg (standard deviation, SD = 0.038 and coefficient of variation, CV = 0.019) for diploid samples (Fig. 5) to 2C = 2.92 pg (standard deviation, SD = 0.048 and coefficient of variation, CV = 0.016) in the tetraploid samples (Fig. 5). The fluorescence peaks using *S. lycopersicum* as a standard overlapped with the peaks of *Adenium* diploid but not with the poliploid variety. The *P. sativum* standard was more appropriate for estimating the DNA content in the polyploid variety due to its high value. To confirm all the DNA C-values, we also used a third standard (*R. sativus*), including replicates. This difference of 68% observed in the tetraploid samples was close to the difference observed in the chromosome measurements, considering a coefficient of variation < 5%. This percentage was maintained in the three additional readings performed with both the diploid and tetraploid samples, always compared with the standards.

Distribution of CMA/DAPI bands in nuclei and chromosomes

The CMA/DAPI banding analyses showed interphase nuclei containing chromocenters $DAPI^+$ (AT-rich regions) with CMA^+ signals (GC-rich regions) arranged at the periphery of the chromocenters (Figs. 6C, 6F, 6G, and 6H). $DAPI^+$ signals were predominant at the pericentromeric regions of 12 chromosomes in the diploid (Fig. 6D). CMA^+ signals were found in the distal regions of six chromosomes. Of those, four signals were larger and brighter, and two were smaller in size (Fig. 6E). In the tetraploid samples, the $DAPI^+$ signals also occurred at the pericentromeric region (Figs. 6I and 6K) adjacent to the CMA^+ in the proximal regions of the six chromosomes (Figs. 6J and 6K).

Cytogenomic analysis

The search for repetitive sequences in the diploid of *A. obesum* (ERX4839710) highlighted the prevalence of LTR-retrotransposons. Approximately 23% of the dataset was composed of sequences from the Gypsy superfamily (Fig. 7A). The remaining lineages were less accumulated, such as the Copia superfamily (< 10%), non-LTRs (> 10%), ERVS (< 6%), and transposons (~20%) (Fig. 7A).The elements of Ogre (superfamily Gypsy) and Ale (superfamily Copia) lineages being the most accumulated (Fig. 7B). Sequences from 35 and 5S rDNA were also estimated, composing ~2% of the dataset (Figs. 7A and 7B). Four putative satellite sequences were identified by the TAREAN tool, but the percentage of satDNAs in the genome was extremely low, ranging from 0.016% to 0.4% (Fig. 8).

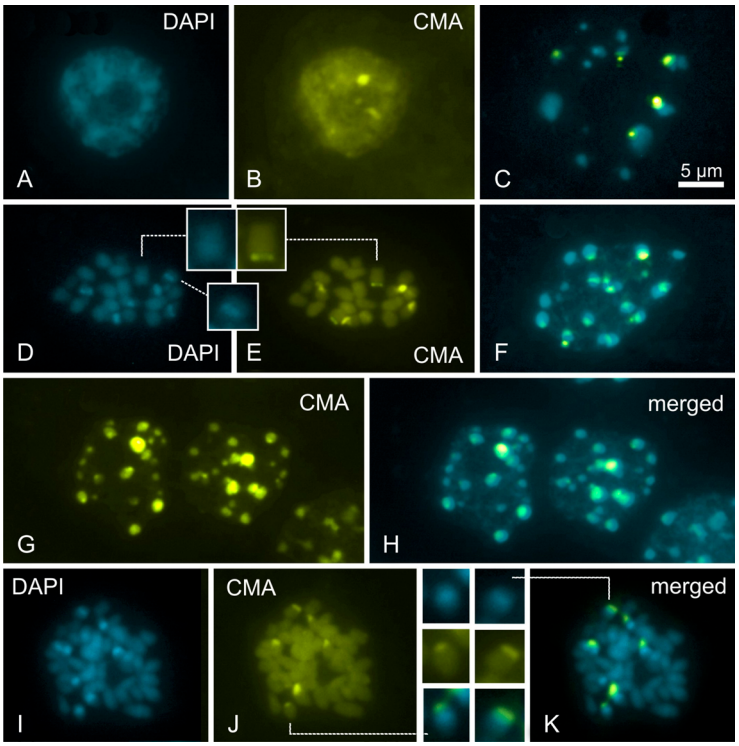

Fig. 6. DAPI (showing AT-rich regions in blue) and CMA (GC-rich regions in greenish yellow) banding analysis in diploid and tetraploid samples of *A. obesum*. (6A and 6C) Interphase nuclei with DAPI$^+$ signals organizing AT-rich chromocenters and (6B and 6C) CMA$^+$ signals showing adjacent GC-rich regions in the diploid. Mitotic metaphase in the diploid showing proximal AT-rich regions and terminal GC-rich bands. The boxes show two different chromosomes with a proximal DAPI band and a distal CMA band. (6F) Merged banding in the tetraploid sample. (6F and 6H) CMA$^+$ signals are located at the periphery of DAPI-stained chromocenters. (6I) Proximal DAPI$^+$ signals in metaphase, (6J) CMA$^+$ bands and (6K) proximal DAPI$^+$ with adjacent CMA$^+$ signals. The boxes show in more detail two different chromosomes with a proximal DAPI band and a distal CMA band. The bar represents 5 µm.

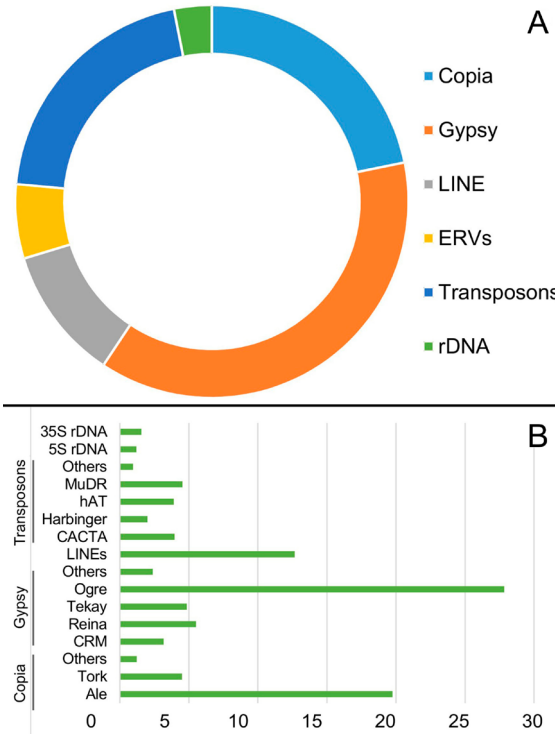

Fig. 7. Estimation of the repetitive DNA portion in the *A. obesum* (diploid) genome. (7A) Retrotransposon LTR sequences were the most accumulated, followed by transposons, ERVs and rDNA. (7B) Among LTR-RTs, the occurrence of Gypsy and Copia superfamilies was similar, with a predominance of Ogre and Ale lineages. For non-LTRs, the most accumulated sequences were LINEs.

Cluster	Proportion[%]	Proportion adjusted[%]	Number of reads	Satellite probability	Consensus length	Consensus	Graph layout
35	0.25	0.25	1701	6.1e-08	513	CAACAATTTTTTACGACAAACTCTCTCGAATTGTAAGTTTATGTAACTTCTATTAAGAGTAATGATGTTGCGTAAATTAT TATTAGTAATGACATTCATTTTTAATTTTTTTAATTGAATCCATCACAAATCAATCATAAATATTGGACTTTTTCAAAAT ATCATTTGATTGTAAAATTTACATAATTTTTTTACAACACTCTCCAATTGTCAGTATGTATATTACTTCTATTAAGAGTA ATTTCTTTGCACAAATTTTTGTTCAAAACGGAGAAGAAAAAGTGGCTGAAAAACAAGAGATATTAAAAATCTGTTGCAAT CCGTGATGGATTTTGCTATATGGTTAACATTTTAAATTTTTTTAATTGAATCGGCTACAAATCTATCGCCAACCCATAGA AATCTACAATGGATTTATGAGGACTTATTTATTTTATTTTTTAATTGAATTCATCGCAAATTAGTCAAAAATGTCGCATT TTTTTTGAAATATCATTTGATTATGGAAAGTTA	

Fig. 8. Satellite DNA sequence obtained from TAREAN that has been detected in the diploid genome. However, it did not produce reproducible signals in after FISH assays.

FISH assays using the 35S rDNA probe showed distal hybridization signals in two chromosome pairs in the diploid and three pairs in the tetraploid (Figs. 9A, 9B, 9D and 9F). The hybridization signals observed in the diploid exhibited different sizes, with one pair being larger than the other (Fig. 9B) and located adjacent to or outside chromocenters in interphases (Fig. 9A). In contrast, in the tetraploid, two of the six signals were more intense than the other four (Figs. 9D and 9F). Apparently, 35S rDNA hybridization signals were on the chromocenter edges (Fig. 9D). Several rounds of FISH using the 5S rDNA probe resulted in the most difficult detection in this material. Despite obtaining hybridization signals in interphase, we were unable to detect them in metaphase. FISH signals of the 5S rDNA probe were in the chromocenters in the diploid, i.e. four hybridization sites (Fig. 9C) and in the tetraploid, with eight sites (Fig. 9G). Several attempts of FISH assays were performed with different probes derived from the two main satDNA, CL10 and CL33, but the results were not reproducible enough to describe them, due to low accumulation of satDNA monomers in the genome (see the sequences, Fig. 8). When we used the Gypsy probe in FISH, dispersed signals were observed in part of the chromosomes, and accumulated in the chromocenters, in both diploid and tetraploid samples (Figs. 9H and 9L). When we combine the cytogenomic data from both diploid and tetraploid in a comparative analysis, it becomes clear that there are many more differences than similarities. They differ in the number, size and shape of chromosomes, nuclear DNA content and the number of fluorescent signals generated by DAPI staining and FISH with the 35S rDNA probe. They are similar in the accumulation of 5S rDNA signals and the large number of AT-rich chromocenters, labelled DAPI$^+$. This comparison is shown in Figure 10.

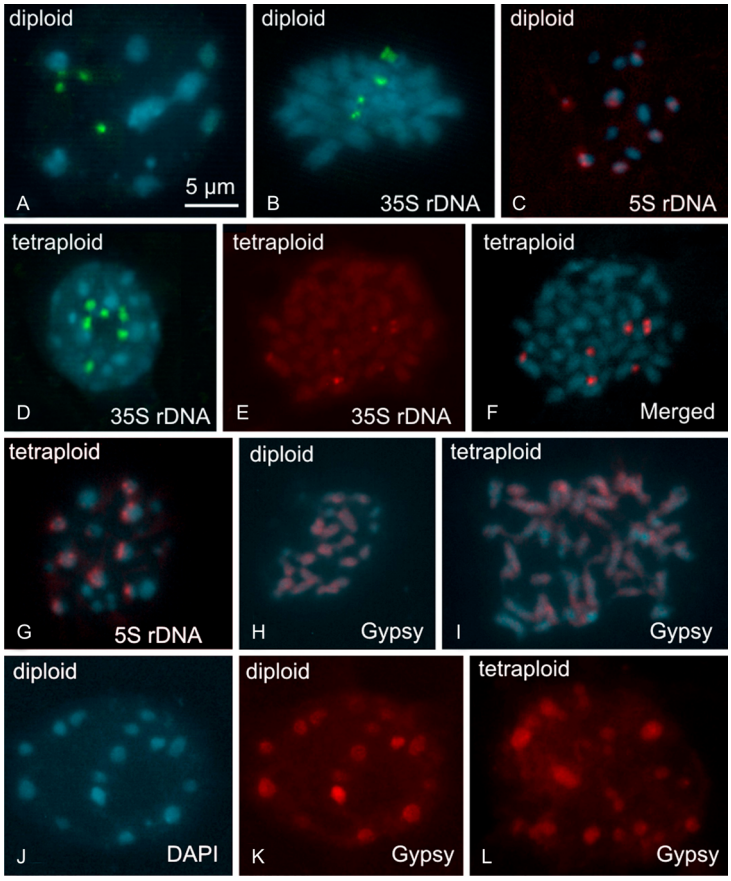

Fig. 9. Fluorescence *in situ* hybridization in nuclei and mitotic chromosomes of diploid and tetraploid samples of *Adenium*, using rDNA and Gypsy probes. (9A) Interphase nucleus showing FISH signals with a 35S rDNA probe on the periphery of the chromocenters, including a larger signal further away from them. (9B) FISH signals with the 35S rDNA probe in the mitotic chromosomes of the diploid sample, showing four distal signals. (9C) Interphase nucleus showing FISH signals with a 5S rDNA probe associated with the chromocenters. (9D) Interphase nucleus showing FISH signals with a 35S rDNA probe inside the nucleus. (9E and 9F) FISH signals with the 35S rDNA probe in the mitotic chromosomes of the tetraploid sample, showing six distal signals. (9G) Interphase nucleus of a tetraploid sample showing FISH signals with a 5S rDNA probe associated with approximately eight chromocenters. (9H and 9I) FISH using a probe for the Gypsy retrotransposon based on a conserved fragment of reverse transcriptase, showing dispersed signals (red) in the diploid and tetraploid chromosomes (blue). (9J and 9L) FISH with Gypsy probe showing signals accumulated in the chromocenters of interphase nuclei of diploid and tetraploid samples. The bar represents 5 µm.

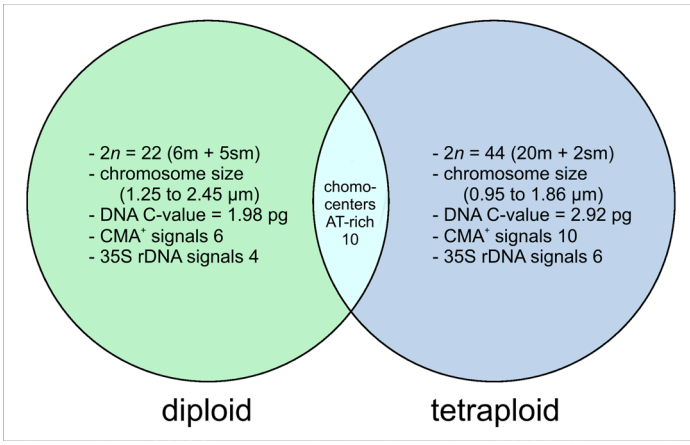

Fig. 10. Venn diagram comparing the main cytological and genomic characteristics of diploid (*A. obseum*) and tetraploid (*A. arabicum*) samples. It shows that there are more differences than similarities between them.

Discussion

Cytogenetics in Apocynaceae and Adenium

According to Dimmitt and Edwards (2021), *Adenium arabicum* populations are morphologically variable, ranging from shrubs to trees, with flowers varying in both shape and size. These authors also report that this tetraploid species rarely hybridizes with any other *Adenium* taxon in cultivation. This reinforces the fact that when there is reproductive isolation between two taxonomic entities, they can be considered distinct, even if they are morphologically similar. Our results showed that in addition to differences in chromosome numbers, chromosome size was variable, ranging from 1.25 to 2.45 µm in the diploid and from 0.93 to 1.86 µm in the tetraploid. These data differ from those reported by Das et al. (1999), which may be related to measurements made with metaphases at different levels of condensation.

Comparative cytogenomics, which uses data on chromosome number and morphology, karyotype organization, meiosis, and DNA C-value estimates, has the potential to discriminate between species and chromosomal races (Liehr, 2021). The importance of using these tools in botanic groups that are neglected or have scarce cytogenetic information, such as Apocynaceae, is even greater. Species from Apocynaceae have small chromosomes, which make them difficult to analyze (Endress et al., 2014). According to Van der Laan and Arends (1985), the chromosome size in Apocynaceae ranges from 0.5 µm to 3.5 µm, presenting meta and submetacentric chromosomes. The Apocynoidae subfamily is considered paraphyletic, with karyotypes numerically stable with $2n = 22$, such as described for species from the *Nerium* (Ebrahimi et al. 2021), resembling *Adenium*. In our analysis, both diploid ($2n = 2x = 22$) and tetraploid ($2n = 4x = 44$) varieties exhibited small chromosomes, from meta- to submetacentric types and relatively symmetrical karyotypes, which agrees in part with previous publications (Van der Laan and Arends, 1985). If we consider $x = 11$ as the basic chromosome number for the Nerieae tribe, *A. swazicum* G.D. Rowley would also be tetraploid with $2n = 2x = 44$, as would the tetraploid *A. obesum* (or *A. arabicum*).

The DNA C-value in Apocynaceae ranges from 2C = 0.60 pg in the genus *Apocynum* L. (Bai et al., 2012) to 2C = 4.90 pg in *Hoodia gordonii* Masson (Zonneveld et al., 2005). Our estimates of 2C = 1.98 pg for the diploid and 2C = 2.92 pg for the tetraploid are compatible with those observed in Apocynaceae. The differences between our results and those of Das et al. (1999), with 4C = 12.76 pg for *A. arabicum* and 13.94 pg for *A. obesum*, can be explained by methodological details, such as sample preparation, hydrolysis time, and type of tissue analyzed. In any case, the data obtained by Das and colleagues refer to samples with the same ploidy level, differing from our sample of the tetraploid variety. The combination of flow cytometry and other techniques is critical, especially when comparing diploid and polyploid genomes, or when differences occur due to high accumulation of repetitive sequences (Pellicer and Leitch, 2020).

Plant genomes may be tolerant to increase DNA content via whole genome duplication. Polyploidy can lead to the development of unique genetic traits that can help to survive under unfavorable conditions, especially for natural polyploids (Basit and Lim, 2024). Although polyploidy makes it possible to restore the fertility status of sterile crosses, it can create a barrier to the success of new interspecific crosses and, in some cases, it can lead to the process of speciation. Regarding the diploid and tetraploid *A. obesum*, this increase has also been observed in plant sizes, where the polyploid presented an expansion of vegetative parts. Besides, these diploid ($2n = 22$) and tetraploid ($2n = 44$) karyotypes were asymmetrical and similar in interphase nuclei morphology, in terms of chromocenter organization.

Complete genome duplications culminating in polyploids are common in plant differentiation and speciation and occur in most angiosperms (Heslop-Harrison et al., 2023). The results presented here indicate that tetraploid samples have smaller chromosome sizes and DNA C-values than related diploids. Analysis of genome size by flow cytometry allows the detection of genomic changes, particularly in the presence of polyploidy. It has been used in ornamental plants (Mujib et al., 2023), as well as to study the taxonomy, evolution, and genetics of other plant groups such as *Passiflora* (Ferreira et al., 2020). In general, these variations are caused by numerical chromosomal rearrangements, such as polyploidy, but also by copy number gain or loss of repetitive DNA sequences, as reported in *Eleocharis*, Cyperaceae (Souza et al., 2025). Differences in the DNA C-value observed between the diploid and tetraploid *A. obsesum* suggest that they are distinct taxonomic entities. It is also important to mention that there is a geographical separation, where *A. arabicum* (tetraploid taxa) can be found in drier areas of northern South Africa (more severe climatic conditions), while diploid *A. obesum* occurs in more humid areas of sub-Saharan Africa (Dimmit and Edwards, 2021).

Organization of repetitive DNA in Adenium

The most portion of plant genomes is composed of repetitive sequences, mainly transposable elements (Ramakrishnan et al., 2022). The same genomic organization was found here in the partially sequenced genome of diploid *A. obesum.* Some studies in other Apocynaceae point out that this fraction occupies 51.65% of *Asclepias syriaca*, while in *Hancornia speciosa,* it represents 19.87%, by transposable elements (Santos et al., 2020). The chromocenters found in both diploid and tetraploid samples of *A. obesum*, which are $DAPI^+$ (AT-rich) with CMA^+ (GC-rich) signals at their borders, are hotspots for repetitive DNA accumulation. According to Feng and Michaels (2015), chromocenters may be defined cytologically as condensed bodies in interphasic nuclei, which are rich in repetitive DNA sequences, such as satDNA and TEs. But the presence of $DAPI^+$ chromocenters does not always mean that we will find large AT-rich heterochromatic blocks in the chromosomes, such as mentioned by Montenegro et al. (2023) in *Citrus*. The distribution of $DAPI^+$ and CMA^+ bands was also similar in the diploid and tetraploid samples of *A. obseum*, the number of bands in the tetraploid chromosome varied. Our findings showed that these AT-rich chromocenters also contain Gypsy retrotransposon sequences. Chromocenter rich in repetitive DNA sequences were also revealed by FISH in the interphase nuclei of *Coffea* species (Cintra et al., 2021).

In the context of repetitive DNA, transposable elements may be important in *Adenium* production because they can affect the diversity of phenotypes (Hassan et al., 2023). Although data on chromosome banding in Apocynaceae are scarce, in *Catharanthus roseus*, constitutive heterochromatin can be found in 20% of the genome, with $DAPI^+$ bands predominating in the pericentromeric regions (Guimarães et al., 2012). Our results on the location of satDNA in *Adenium* were unsuccessful because these sequences represent only about 0.7% of the genome.

FISH using rDNA probes in both diploid and tetraploid samples showed hybridization sites in the distal chromosome regions, with variation in the number of FISH signals. Such variation is common in angiosperms (see Assis et al. 2023). Although the numbers of hybridization sites between diploid and tetraploid differed, each FISH signal was linked to chromocenters, associated with CMA^+ bands. Similar associations have been observed in *Tulbaghia* of Amaryllidaceae (Báez et al., 2020) and *Dorstenia* of the Moraceae family (Barreto et al., 2023). Our data shows that different repetitive DNA families are involved in chromocentric organization, such as in nuclei of *Coffea* species, unlike the 35S rDNA sequences that were located in their peripheral regions. These results suggest that repetitive DNA sequences are maintained in *Adenium* chromosomes in a non-random distribution, similar to that in other plant species.

Conclusions

The cytogenomic analyses performed here confirm that there are more differences than similarities between the diploid (relative to *A. obesum*) and tetraploid (*A. arabicum*) samples. These data are sufficient to rule out the possibility that these are varieties of *A. obesum* and thus accept them as two independent species. These results agree with the phylogenetic data published by Dimmitt and Edwards (2021), where *A. obesum* and *A. arabicum* appear in different clades. Future studies to understand the role of the repetitive DNA fraction in generating floral diversity in this group of ornamentals are promising. These data add to our knowledge of the genetics of these plants and could enable biotechnological advances in desert rose breeding.

Acknowledgments

Juliana Machado da Silva, Talita Angélica de Oliveira Rosa, Letícia Maria Parteka, Rafael de Assis, and Thamirys Silva Valentim are grateful for the fellowships from CAPES and CNPq. André Luis Laforga Vanzela is grateful for financial support from the Brazilian Agency CNPq (processes 407194/2018-5 and 309902/2018-5). The authors also thank ProPPG-UEL, PPG-GBM, FINEP, and Fundação Araucária for other types of support.

Author Contribution

TAOR: Data Curation, Formal Analysis, Investigation, Writing – Original Draf. **JMS:** Data Curation, Formal Analysis, Investigation, Writing – Original Draf. **TSV:** Data Curation, Formal Analysis, Investigation, Writing – Original Draf. **RA:** Formal Analysis**. LMP:** Data Curation, Formal Analysis, Investigation, Writing – Original Draf. **ALLV:** Conceptualization, Funding Acquisition, Formal Analysis, Resources, Supervision, Writing - Review & Editing.

Conflict of Interest

The authors declare that they have no known competing financial interests or personal relationships that could have appeared to influence the work reported in this paper.

Data Availability Statement

All the research data is contained in the manuscript.

Declaration of generative AI and AI-assisted technologies in the writing process

The authors declare that the use of AI and AI-assisted technologies was not applied in the writing process.

References

ASSIS, R.; GONÇALVES, L.S.A.; GUYOT, R.; VANZELA, A.L.L. Abundance of distal repetitive DNA sequences in *Capsicum* L. (Solanaceae) chromosomes. **Genome**, v.66, n.10, 2023. https://doi.org/10.1139/gen-2022-0083

BAI, C.; ALVERSON, W.S.; FOLLANSBEE, A.; WALLER, D.M. New reports of nuclear DNA content for 407 vascular plant taxa from the United States. **Annals of Botany**, v.110, n.8, p.1623-1629, 2012. https://doi.org/10.1093/aob/mcs222

BÁEZ, M.; SOUZA, G.; GUERRA, M. Genome size and cytomolecular diversification in two species of the South African endemic genus *Tulbaghia* L. (Allioideae, Amaryllidaceae). **South African Journal of Botany**, v.130, p.407-413, 2020. https://doi.org/10.1016/j.sajb.2020.01.024

BARRETO, L.M.; ASSIS, R.; VANZELA, A.L.L. Chromosomal and genomic data in Neotropical *Dorstenia* species (Moraceae) and their relationships with African species. **Botanical Journal of the Linnean Society**, v.202, n.1, p.76-92, 2023. https://doi.org/10.1093/botlinnean/boac076

BASIT, A. and LIM, K-B. Systematic approach of polyploidy as an evolutionary genetic and genomic phenomenon in horticultural crops. **Plant Science** v.348, p.112236, 2024. https://doi.org/10.1016/j.plantsci.2024.112236

CINTRA, L.A.; SOUZA, T.B.; PARTEKA, L.M.; BARRETO, L.M.; PEREIRA, L.F.P.; GAETA, M.L.; GUYOT, R.; VANZELA, A.L.L. An 82 bp tandem repeat family typical of 30 non-coding end of Gypsy/TAT LTR retrotransposons is conserved in *Coffea* spp. pericentromeres. **Genome**, v.65, n.3, 2021. https://doi.org/10.1139/gen-2021-0045

COLOMBO, R.C.; CRUZ, M.A.; CARVALHO, D.U.; HOSHINO, R.T.; ALVES, G.A.C.; FARIA, R.T. *Adenium obesum* as a new potted flower: growth management. **Ornamental Horticulture**, v.24, n.3, p.197-205, 2018. https://doi.org/10.14295/oh.v24i3.1226

DAS, A.B.; MOHANTY, S.; DAS, P. Chromosome number, karyotype, and nuclear DNA content in some *Adenium* species of the family Apocynaceae. **Cytobios**, v.98, n.388, p.95-104, 1999.

DIMMITT, M.; EDWARDS, T. *Adenium* Taxonomy and Nomenclature: Progress Creates More Questions. **Cactus and Succulent Journal**, v.93, n.4, p.252-266, 2021. https://doi.org/10.2985/015.093.0401

EBRAHIMI, F.; NOHOOJI, M.G.; MIRI, S.M. First karyotype analysis of *Nerium oleander* populations in Iran. **Rostaniha**, v.22, n.2, p.186-193, 2021. https://doi.org/10.22092/botany.2021.354571.1246

ENDRESS, M.E.; LIEDE-SCHUMANN, S.; MEVE, U. An updated classification for Apocynaceae. **Phytotaxa**, v.159, n.3, p.175-194, 2014. http://dx.doi.org/10.11646/phytotaxa.159.3.2

FENG, W.; MICHAELS, S.D. Accessing the inaccessible: The organization, transcription, replication, and repair of heterochromatin in plants. **The Annual Review of Genetics**, v.49, n.1, p.439-459, 2015. https://doi.org/10.1146/annurev-genet-112414-055048

FERREIRA, D.A.T.; PRAÇA-FONTES, M.M.; VIEIRA, A.T.; NUNES, A.C.P.; CLARINDO, W.R. Karyotype and nuclear DNA content variation in *Passiflora* L. **Scientia Horticulturae**, v.272, 109532, 2020. https://doi.org/10.1016/j.scienta.2020.109532

FISHBEIN, M.; LIVSHULTZ, T.; STRAUB, S.C.K.; SIMÕES, A.O.; BOUTTE, J.; MCDONNELL, A.; FOOTE, A. Evolution on the backbone: Apocynaceae phylogenomics and new perspectives on growth forms, flowers, and fruits. **American Journal of Botany**, v.105, n.3, p.495-513, 2018. https://doi.org/10.1002/ajb2.1067

GUIMARÃES, G.; CARDOSO, L.; OLIVEIRA, H.; SANTOS, C.; DUARTE, P.; SOTTOMAYOR, M. Cytogenetic characterization and genome size of the medicinal plant *Catharanthus roseus* (L.) G. Don. **AoBP Plants**, v.2012, p.pls002, 2012. https://doi.org/10.1093/aobpla/pls002

HASSAN, A.H.; MOKHTAR, M.M.; EL ALLALI, A. Transposable elements: multifunctional players in the plant genome. **Frontiers in Plant Science**, v.14, p.1330127, 2023. https://doi.org/10.3389/fpls.2023.1330127

HASTUTI, D.; SURANTO, S.; SETYONO, P. Variation of morphology, karyotype, and protein band pattern of *Adenium* (*Adenium obesum*) varieties. **Nusantara Bioscience**, v.1, n.2, p.78-83, 2009. https://doi.org/10.13057/nusbiosci/n010205

HESLOP-HARRISON, J.S.; SCHWARZACHER, T.; LIU, Q. Polyploidy: its consequences and enabling role in plant diversification and evolution. **Annals of Botany**, v.131, n.1, p.1-10, 2023. https://doi.org/10.1093/aob/mcac132

LIEHR, T. Molecular cytogenetics in the era of chromosomic and cytogenomic approaches. **Frontiers in Genetics**, v.12, p.720507, 2021. https://doi.org/10.3389/fgene.2021.720507

MONTENEGRO, C.; ROA, F.; FILHO, W.S.S.; SILVA, A.E.B. Heterochromatic patterns of *Citrus* revisited: a new look at species origins and karyotype evolution. **Tree Genetics & Genomes**, v.19, p.36, 2023. https://doi.org/10.1007/s11295-023-01610-0

MUJIB, A., MAMGAIN, J., BANSAL, Y., EJAZ, E. Interspecific genome size (2C DNA) variation in some ornamental and medicinal plants: Is it a phenomenon of partial sequence amplification or loss? **In Genome size and genetic homogeneity of regenerated plants**, 2023. p. 327-351.

NOVAK, P.; ROBLEDILLO, L.A.; KOBLIZKOVA, A.; VRBOVA, I.; NEUMANN, P.; MACAS, J. TAREAN: a computational tool for identification and characterization of satellite DNA from unassembled short reads. **Nucleic Acids Research**, v.45, n.12, p.e111, 2017. https://doi.org/10.1093/nar/gkx257

PELLICER, J.; LEITCH, I. The Plant DNA C-values database (release 7.1). **The New Phytologist**, v.226, n.2, p.301-305, 2020. https://www.jstor.org/stable/26914539

PRAÇA-FONTES, M.M.; CARVALHO, C.R.; CLARINDO, W.R.; CRUZ, C.D. Revisiting the DNA C-values of the genome size-standards used in plant flow cytometry to choose the ‘‘best primary standards’. **Plant Cell Reports** v.30, p.1183-1191. 2011. https://doi.org/10.1007/s00299-011-1026-x

RAMAKRISHNAN, M.; SATISH, L.; SHARMA, A.; VINOD, K.K.; EMAMVERDIAN, A.; ZHOU, M.; WEI, Q. Transposable elements in plants: Recent advancements, tools and prospects. **Plant Molecular Biology Reports**, v.40, p.628-645, 2022. https://doi.org/10.1007/s11105-022-01342-w

SANTOS, V.; SILVA, E.F.; ALMEIDA, C. Genome size and identification of repetitive DNA sequences using low coverage sequencing in *Hancornia speciosa* Gomes (Apocynaceae: Gentianales). **Genetics and Molecular Biology**, v.43, n.4, p.e20190175, 2020. https://doi.org/10.1590/1678-4685-GMB-2019-0175

SCHENK, J.J.; BECKLUND, L.E.; CAREY, S.J.; FABRE, P.P. What is the “modified” CTAB protocol? Characterizing modifications to the CTAB DNA extraction protocol. **Applications in Plant Sciences**, v.11, p.e11517, 2023. https://doi.org/10.1002/aps3.11517

SOUZA, T.B.; GAETA, M.L.; MARTINS, C.; VANZELA, A.L.L. IGS sequences in *Cestrum* present AT- and GC-rich conserved domains, with strong regulatory potential for 5S rDNA. **Molecular Biology Reports**, v.47, p.55-66, 2020. https://doi.org/10.1007/s11033-019-05104-y

SOUZA, T.B.; PARTEKA, L.M.; KUOB, Y.; NASCIMENTO, T.; SCHUBERT, V.; PEDROSA-HARAND, A.; MARQUES, A.; HOUBEN, A.; VANZELA, A.L.L. . Distinct patterns of satDNA distribution in holocentric chromosomes of spike-sedges (*Eleocharis*, Cyperaceae). **Genome**, v. 68, p. 1-13, 2025. https://dx.doi.org/10.1139/gen-2024-0089

TEMSCH, E.M.; KOUTECKÝ, P.; URFUS, T.; ŠMARDA, P.; DOLEŽEL J. Reference standards for flow cytometric estimation of absolute nuclear DNA content in plants. **Cytometry**, v. 101, p.710-724, 2022. https://doi.org/10.1002/cyto.a.24495

VAN DER LAAN, F.M.; ARENDS, J.C. Cytotaxonomy of the apocynaceae. **Genetica**, v.68, n.1, p.3-35, 1985. https://doi.org/10.1007/BF02424563

VIMALA, Y.; LAVANIA, S.; LLAVANIA, U.C. Chromosome change and karyotype differentiation–implications in speciation and plant systematics. **Nucleus**, v.64, p.33-54, 2021. https://doi.org/10.1007/s13237-020-00343-y

ZONNEVELD, B.J.M.; LEITCH, I.J.; BENNETT, M.D. First nuclear DNA amounts in more than 300 Angiosperms. **Annals of Botany**, v.96, n.2, p.229-244, 2005. https://doi.org/10.1093/aob/mci170